

# Device-independent quantum key distribution with single-photon sources

A. Máttar,<sup>1</sup> J. Kołodyński,<sup>1</sup> P. Skrzypczyk,<sup>2</sup> D. Cavalcanti,<sup>1</sup> K. Banaszek,<sup>3,4</sup> and A. Acín<sup>1,5</sup>

<sup>1</sup>*ICFO-Institut de Ciències Fotoniques, The Barcelona Institute of Science and Technology, 08860 Castelldefels (Barcelona), Spain*

<sup>2</sup>*H. H. Wills Physics Laboratory, University of Bristol, Tyndall Avenue, Bristol, BS8 1TL, United Kingdom*

<sup>3</sup>*Faculty of Physics, University of Warsaw, Pasteura 5, 02-093 Warszawa, Poland*

<sup>4</sup>*Centre of New Technologies, University of Warsaw, Banacha 2c, 02-097 Warszawa, Poland*

<sup>5</sup>*ICREA-Institució Catalana de Recerca i Estudis Avançats, Lluís Companys 23, 08010 Barcelona, Spain*

Device-independent quantum key distribution protocols allow two honest users to establish a secret key with minimal levels of trust on the provider, as security is proven without any assumption on the inner working of the devices used for the distribution. Unfortunately, the implementation of these protocols is challenging, as it requires the observation of a large Bell inequality violation between the two distant users. Here, we introduce novel photonic protocols for device-independent quantum key distribution exploiting single-photon sources and heralding-type architectures. The heralding process is designed so that transmission losses become irrelevant for security. We then show how the use of single-photon sources for entanglement distribution in these architectures, instead of standard entangled-pair generation schemes, provides significant improvements on the attainable key rates and distances over previous proposals. Given the current progress in single-photon sources, our work opens up a promising avenue for device-independent quantum distribution implementations.

The paradigm of *device-independent quantum key distribution* (DIQKD) offers the strongest form of secure communication, relying only on the validity of quantum mechanics, but not on any detailed description, or trust, of the inner workings of the users devices.<sup>1–3</sup> On the theoretical side, the security of DIQKD has been proven against increasingly powerful eavesdroppers,<sup>4,5</sup> culminating in proofs of security against attacks of the most general form.<sup>6,7</sup>

The main challenge facing experimental DIQKD are its stringent demands on the observable data, necessary for the security requirements to be met. First, any DIQKD implementation should be based on the observation of data that conclusively violates a Bell inequality.<sup>8,9</sup> In particular, the Bell experiment should close the so-called ‘detection loophole’,<sup>10</sup> otherwise, hacking attacks can fake a violation at the level of the detected events when losses are high enough.<sup>11</sup> Moreover, a detection-loophole-free Bell violation is necessary but not sufficient for secure DIQKD, as the necessary detection efficiencies are significantly higher than those required for Bell violation. For instance, while the detection efficiency for observing a Bell violation of the Clauser-Horne-Shimony-Holt (CHSH)<sup>12</sup> inequality can be as low as  $2/3$ ,<sup>13</sup> a DIQKD protocol based on CHSH requires an efficiency of the order of 90%.<sup>3</sup> This is, in fact, a general feature of any noise parameter—consider, e.g., the visibility<sup>4</sup>—that affects not only the observed Bell violation, but also the correlations between the users aiming to construct the secret key.

The first Bell experiments closing the detection loophole used massive particles.<sup>14–17</sup> Leaving aside table-top<sup>14,15</sup> and short-distance<sup>16</sup> experiments, the Bell test of Hensen *et al.*<sup>17</sup> involved labs separated by a distance of 1.3 km, which allowed to close also

the ‘locality loophole’.<sup>9</sup> Nevertheless, as the employed light-matter interaction processes typically deteriorate the quality of the nonlocal correlations generated between the users, the reported violations would not have been sufficient for secure DIQKD. Furthermore, the rates of key distribution they could provide are seriously limited owing to the measurements involved that, despite allowing for near unit efficiency, take significant time.<sup>18,19</sup> While improvements are to be expected in all these issues, and massive particles may be essential for long-distance schemes involving quantum repeaters,<sup>20</sup> photon-based schemes appear more suitable to obtain high key rates with current or near-future technology. Photonic losses, however, occurring at all of the generation, transmission, and detection stages represent the main challenge in these schemes. Recent advances have been made for photo-detection efficiencies, which allowed for the first loophole-free photonic Bell inequality violations over short distances.<sup>21–24</sup> Still, not only are the reported distances far from any cryptographic use, but also the observed Bell violations are again not large enough for secure DIQKD.

In this work, we show that single-photon sources<sup>25</sup> constitute a promising resource for experimental photonic DIQKD. Such sources have already allowed for nearly on-demand,<sup>26</sup> highly efficient<sup>27</sup> extraction of single photons (also in pulse trains<sup>28,29</sup> as well as at telecom wavelengths<sup>30</sup>), while maintaining their purity and indistinguishability even above the 99% level.<sup>31,32</sup> We propose novel DIQKD photonic schemes that thanks to the replacement of the photon-pair creation process (achieved, e.g., by parametric downconversion<sup>33</sup>) with single-photon sources allow to distribute the key at significant rates over large distances. We believe that, in view of the recent

advances in the fabrication of single-photon sources, our results point out a promising avenue for DIQKD implementations.

### Overcoming transmission losses by heralding

From a cryptographic perspective, the photonic losses in optical Bell experiments should be divided into two categories. Losses that occur within the local surroundings—laboratories—of the users who aim at establishing the secret key should be differentiated from those that occur during the photon transmission between the labs.

Concerning local losses, we parametrise them by the effective *local efficiency*,  $\eta_l$ , which accounts for all photon-loss mechanisms inside the lab, including imperfect photo-detection, any optical path and mode mismatch, finite photon-extraction efficiency of the sources locally employed by a user, etc. To our knowledge, all known DIQKD protocols require a high local efficiency, of the order of 90%. While the existence of practical DIQKD protocols tolerating lower local efficiencies cannot be excluded, we don't expect any significant improvement in this direction. To achieve high enough local efficiencies is in our view a secondary challenge that can be eventually solved by technological development. In fact, we expect Bell experiments with local losses of the order of 90% to be soon within reach. In this work, we work under this assumption, which is at the moment essential for any DIQKD implementation.

The second type of losses occur while photons propagate outside the labs and are effectively quantified by the *transmission efficiency*,  $\eta_t$ , of the channel connecting the users. They constitute the main hurdle for long-distance DIQKD, as  $\eta_t$  decreases exponentially with distance. The only known viable route to prevent transmission losses from opening the detection loophole is to record an additional outcome, denoted by  $\checkmark$ , indicating in a heralded way that the photons did not get lost.<sup>34,35</sup> Then,  $\checkmark$  assures that the required quantum state was successfully transmitted between Alice and Bob and the Bell test can be performed. If the heralding outcome is causally disconnected from the choices of measurement settings  $x, y$  by Alice and Bob during each round of the protocol (see Fig. 1), transmission losses become irrelevant with respect to the security of the protocol, affecting only the key rate.

The heralding process can in principle be implemented with the help of a quantum non-demolition (QND) measurement allowing the number of photons to be measured without disturbing the quantum state.<sup>36</sup> QND photon measurements are, however, challenging, requiring unrealistic non-linearities. The solution is to replace them with optical linear circuits that achieve the same goal in a probabilistic fashion.<sup>37,38</sup> The heralding signal  $\checkmark$  is then provided by a particular detection pattern in the linear optics circuit indicating, as for the QND measurement, that

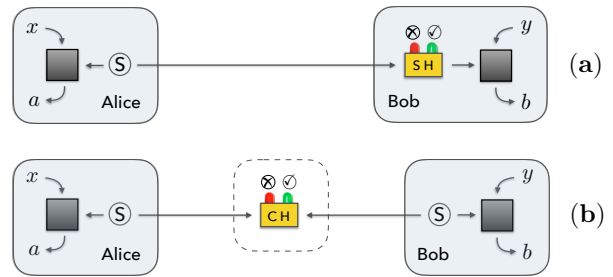


FIG. 1. **Efficient heralding schemes for DIQKD.** Alice and Bob are located at isolated labs (shaded regions) from which they control information leaks. They locally use sources  $S$ , to distribute a quantum state between their labs and perform on it randomly sampled measurements labelled  $x$  and  $y$ , producing outcomes  $a$  and  $b$ . The measurement devices are treated as black-boxes that yield a joint probability distribution  $\mathbf{p} = P(ab|xy)$  compatible with the laws of quantum physics. A *heralding scheme* is implemented, such that, given its positive outcome  $\checkmark$ , the resulting  $p(ab|xy\checkmark)$  shared between Alice and Bob becomes effectively independent of the finite transmission efficiency. In the *side-heralding* (SH) scenario, (a), this is achieved by one of the users performing a (probabilistic) quantum non-demolition measurement (QND) within their isolated lab that verifies the arrival of the distributed state, without disturbing it. In the *central-heralding* (CH) scheme, (b), the heralding is performed by a third party that later publicly announces the successful rounds that should be used during the protocol.

the outputs produced by the Bell test are valid.

Within the *side-heralding* (SH) scenario depicted in Fig. 1(a), the circuit is performed by one of the users who records the rounds in which the positive heralding pattern,  $\checkmark$ , has occurred, so that only these are later used for key extraction. In contrast, in the *central-heralding* (CH) scenario the heralding is performed outside of the users labs, at a central station (resembling the entanglement swapping configuration<sup>39</sup>), by a third party who then publicly announces which rounds should be considered successful, as illustrated in Fig. 1(b). In either case, the heralding scheme should be causally disconnected from the measurements in the Bell test. This condition is more natural in the CH scheme but it may also be assumed in the SH configuration. Moreover, the heralding signal should work as the ideal QND measurement and assure that, up to the leading order, transmission losses have no effect on the heralded Bell violation.

The importance of this requirement is best understood by considering existing proposals for photonic DIQKD that do not satisfy it, such as the schemes using a noiseless qubit amplifier<sup>34</sup> or entanglement swapping relays.<sup>40–42</sup> In all these schemes, entanglement between users is distributed using spontaneous parametric down-conversion<sup>33</sup> (SPDC) sources—a

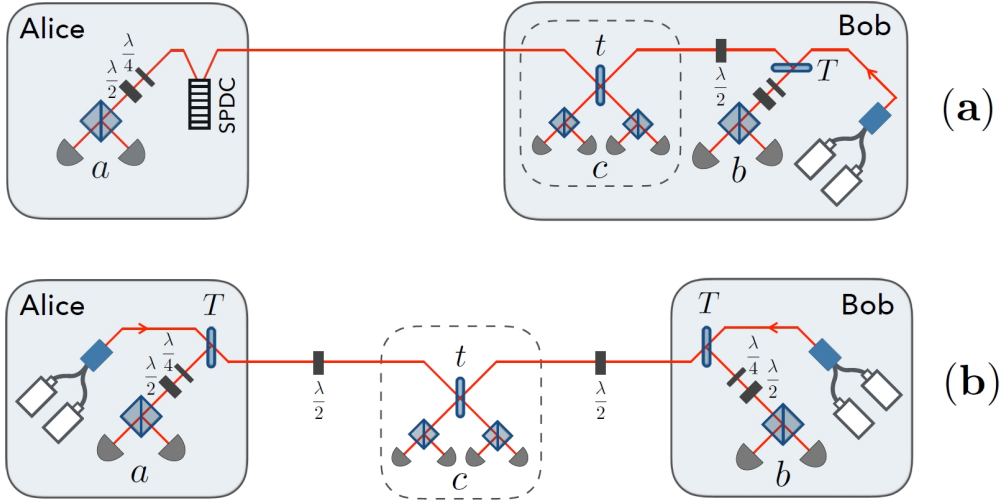


FIG. 2. **DIQKD schemes with single-photon sources.** (a): *Side-heralding (SH) scheme employing two single-photon sources.* The SPDC source is kept close to Alice to avoid transmission losses on her side. Bob impinges two single photons encoded in orthogonal polarizations onto a BS of transmittance  $T \approx 1$  located in his lab (shaded region). The reflected mode is then jointly analysed with the system received from Alice by a partial Bell-state measurement (BSM, dashed region) consisting of: a partial BS of transmittance  $t$ , polarizing-BSs (split squares) and binary on/off photodetectors (half-circles). (b): *Central-heralding (CH) scheme employing two single-photon sources.* Both Alice and Bob impinge two single photons encoded in orthogonal polarizations onto BSs of transmittance  $T \approx 0$  situated in their labs. A partial BSM is conducted this time at the central station on the combined polarization components arriving from Alice and Bob after being passed through HWPs ( $\frac{\lambda}{2}$ ). In both schemes, the users apply their choice of the measurement settings  $x$  and  $y$  on the output modes by means of a polarization analyser—a sequence of a quarter-wave plate ( $\frac{\lambda}{4}$ ), HWP, polarizing BS and two binary detectors.

probabilistic process in which multi-photon pair creation also takes place. For the sake of argument, let us consider the state produced by the SPDC to read:  $|0\rangle\langle 0| + \bar{p}|\psi_{AB}\rangle\langle\psi_{AB}|$ ; after, without loss of generality, ignoring its normalisation and the higher-order terms in  $\bar{p}$ , i.e., the spurious contributions arising when more than one photon-pair is created within the process—see App. A. We discuss in more detail the qubit amplifier of Gisin *et al.*<sup>34</sup> in App. B, yet in all the cases<sup>34,40–42</sup> the state shared by the users after a successful heralding takes a general form (up to irrelevant normalisation):

$$\rho_{AB|\odot} = |0\rangle\langle 0| + \lambda\eta_t\bar{p}|\psi_{AB}\rangle\langle\psi_{AB}| + \dots, \quad (1)$$

in which the detrimental terms of order  $\bar{p}$  that yield deviations from the target  $|\psi_{AB}\rangle$  may also be omitted. The parameter  $\lambda > 0$  above is determined by the particular heralding scheme,<sup>34,40–42</sup> while  $\eta_t$  is the transmission efficiency dependent on the distance between the users. Importantly, the contribution of the maximally entangled state,  $|\psi_{AB}\rangle$ , occurs at a higher order in  $\bar{p}$  than the vacuum contribution. Subsequently, for any fixed  $\lambda$ , the Bell violation strongly depends on  $\eta_t$ —contrary to when performing an ideal QND measurement. As  $\eta_t$  vanishes exponentially with the separation distance  $L$  ( $\eta_t = e^{-L/L_{\text{att}}}$ , with typical values of the attenuation length  $L_{\text{att}} \approx 20$  km), the heralded state (1) approaches the vacuum exponentially with  $L$

and rapidly ceases to produce large enough Bell violations for the detection loophole to be closed, let alone for DIQKD to be possible.<sup>43</sup> In fact, the key rates reported in<sup>34,40–42</sup> are only possible if one makes some extra assumptions about the eavesdropping attacks (see Supp. Mat. of Ref. 34).

In what follows, we propose two DIQKD architectures based on single-photon sources<sup>25</sup> that crucially do not suffer from the above problem, allowing thus for high key rates and large communication distances. One of the schemes relies solely on such sources and a CH-based implementation. Since single-photon sources are still an expensive resource compared to widely used SPDC sources, we also consider a SH-based scheme in which both source-types are used in conjunction. In order to maintain generality and a degree of comparison with the SPDC framework,<sup>33</sup> each single-photon source is modelled to produce a quantum state that, when ignoring normalisation (see App. A), reads  $\sigma_{\text{SP}} = \sum_{n=1}^{\infty} p^{n-1} |n\rangle\langle n|$  in the photon-number basis, containing an infinite tail of high-order contributions whose probability is parametrised by  $p$ .

### DIQKD schemes with single-photon sources

The *SH scheme* requires Bob to produce two single photons with orthogonal polarizations  $H$  and  $V$ , while Alice has access to entangled photon-pairs produced by an SPDC source. It is inspired by the

DIQKD Scheme:	Side-heralding (SH)	Central-heralding (CH)
Critical local efficiency $\eta_l^*$ (diqkd)	94.9%	94.3%
Critical local efficiency $\eta_l^*$ (nonloc.)	74.3%	69.2%
Noise robustness (nonloc.)	31.2%	35.7%
Secret key per heralded round (bit fraction $\leq 1$ )	0.82	0.95

TABLE I. **Performance of DIQKD schemes.** Critical local efficiencies,  $\eta_l^*$ , only above which the secret key can be distributed in a fully device-independent fashion, compared with ones above which the shared correlations exhibit nonlocality. For perfect local efficiencies ( $\eta_l = 1$ ), robustness to mixing the joint probability distribution with a maximally uncorrelated one is listed, as well as the bit fraction of the secret key generated per successfully heralded round, equal to one in the ideal case. The probability of producing a single photon or an SPDC photon-pair is assumed as  $p = \bar{p} = 10^{-4}$  for each source.

qubit-amplifier implementation of Pitkanen *et al.*<sup>43</sup>, as shown in Fig. 2(a). Bob's photons enter a beam-splitter (BS) of transmittance  $T$ . Then, the reflected light component passes through a half-waveplate (HWP) before being detected in conjunction with Alice's transmitted photons via a partial Bell-state measurement (BSM) depicted by the dashed region. The outcome of the BSM,  $c$ , signifies whether the required heralding pattern,  $c = \checkmark$ , has occurred, corresponding to two detector clicks that represent simultaneous detection of orthogonal polarizations.

Provided that the BS transmittance is kept close to one ( $T \approx 1$ ),  $\checkmark$  occurs only when exactly one photon is transmitted by the BS while the other photon is reflected, and the single photon-pair term of the state produced in the SPDC by Alice reaches the BSM. In this manner, the photons distributed to Alice and Bob are prepared with orthogonal polarizations, although the information about their concrete polarization is erased by the partial BSM. The resulting state shared by Alice and Bob conditioned on  $\checkmark$  corresponds to a partially (polarization-) entangled two-qubit state with asymmetry dictated by the BSM transmittance parameter  $t$  (in an unnormalised form):

$$\rho_{AB|\checkmark}^{(\text{SH})} = \frac{\eta_t T (1 - T)}{8} |\psi_{AB}^t\rangle \langle \psi_{AB}^t| + O(\bar{p}), \quad (2)$$

where  $\bar{p}$  parametrises the probability to produce multiple pairs in the SPDC process of Alice (see App. C). The target state  $|\psi_{AB}^t\rangle = |\psi_{AB}^-\rangle + t|\phi_{AB}^-\rangle$  in Eq. (2) is a superposition of Bell states given, in second quantization, by  $|\psi_{AB}^-\rangle = \frac{1}{\sqrt{2}}(a_H^\dagger b_V^\dagger - a_V^\dagger b_H^\dagger)|0\rangle$  and  $|\phi_{AB}^-\rangle = \frac{1}{\sqrt{2}}(a_H^\dagger b_H^\dagger - a_V^\dagger b_V^\dagger)|0\rangle$ .

The CH scheme depicted in Fig. 2(b) requires both Alice and Bob to produce two single photons with orthogonal polarizations  $H$  and  $V$ , inspired by the entanglement distribution scheme of Lasota *et al.*<sup>44</sup>. The photons produced on each side are impinged on two BSs of low transmittance ( $T \approx 0$ ) and transmitted to the central station with low probability. The heralding is again provided by a partial BSM, performed now by a third party, after passing both incoming beams through separate HWPs. The signal

$\checkmark$  is observed only when each party transmits exactly one single photon and in such a case the reflected photons kept by Alice and Bob are again in a partially (polarization-) entangled state with asymmetry determined by the transmittance  $t$  of the partial BSM performed at the central station (see App. C):

$$\rho_{AB|\checkmark}^{(\text{CH})} = \frac{\eta_t T^2 (1 - T)^2}{4} |\psi_{AB}^t\rangle \langle \psi_{AB}^t| + O(p). \quad (3)$$

Unlike previous proposals, see Eq. (1), in the above two schemes the vacuum terms do not emerge after heralding. Moreover, the unnormalised states (2) and (3), to first significant order, are pure and proportional to the transmission efficiency  $\eta_t$ . This guarantees that, after normalisation, the states are independent of  $\eta_t$  (to first order). This, and the use of single-photon sources instead of SPDC, are the crucial ingredients that allow us to achieve significantly higher secret key rates at larger distances than previous proposals.

A second advantage of our schemes is that, by adjusting the transmittance  $t$  of the partial BSM, the entanglement of the target state  $|\psi_{AB}^t\rangle$  can be continuously tuned between the maximally entangled ( $t = 0$ ) and product ( $t = 1$ ) extremes.<sup>13</sup> This can be used to improve the local efficiencies,  $\eta_l$ , required for security.

### Fully DI-secure results

A comparison of the SH and CH schemes performance is given in Table I. Although the SH scheme is simpler, requiring only two single-photon sources, its performance is worse than the CH scheme for all figures of merit considered. From here onwards, we focus on the CH scheme, which defines the ultimate experimental requirements for DIQKD to be possible within our approach. In what follows, we show that this scheme offers reasonable levels of robustness against all relevant noise parameters.

The resistance to noise is estimated using a simple noise model, in which the ideal correlations are mixed with white-noise-correlations with weight  $1 - v$  and  $v$ , and perfect local efficiency ( $\eta_l = 1$ ) is assumed. The CH scheme yields nonlocal correlations up to  $v = 35.7\%$  level of mixing. Concerning imper-



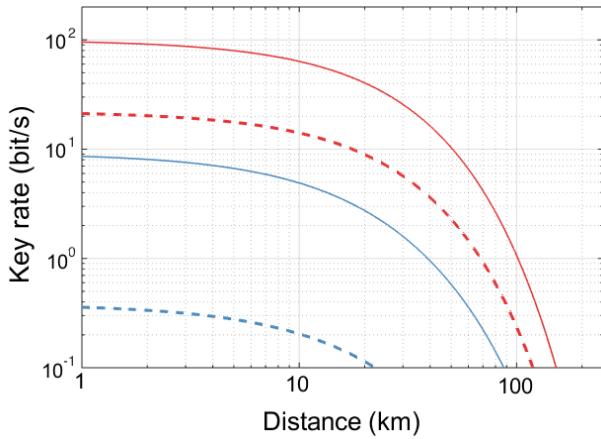


FIG. 3. **DIQKD key rates attained with 95% (blue) and 96% (red) local efficiencies.** In each case, the solid (dashed) curve represents the key rate in bits per second attained by the CH (SH) scheme. Each key rate is optimised over all adjustable physical parameters, yet in the case of the single-photon sources impurity parameter,  $p$ , its lowest possible value is always favoured. Here, we fix  $p = 10^{-4}$  and consider the repetition rate of photon extraction for each source to be 100 MHz.<sup>32</sup>

fection of the single-photon sources, for a realistic<sup>32</sup> value of multi-photon generation of  $p = 10^{-4}$  the CH scheme generates up to 0.95 secret bits per (successfully) heralded round—achieving close to the ultimate limit of 1 secret bit, applicable in a perfectly noiseless scenario.<sup>45</sup> The critical local efficiencies,  $\eta_l^*$  for the nonlocality to be observed are very close to the ultimate bound of Eberhard<sup>13</sup>,  $\eta_l \geq 66.6\%$ , which can be approached due to the ability to prepare pure partially entangled two-qubit states within both the SH and CH schemes.

Most importantly, employing the CH scheme for DIQKD, our work predicts that positive key rates can be generated independently of the separation between Alice and Bob, as long as the effective local efficiency,  $\eta_l$ , for each of the user labs is higher than 94.3%. Assuming  $\eta_l$  to be the product of the efficiencies of photon extraction from each single-photon source employed ( $\eta_{ls}$ ); transmission between the sources and detectors involved ( $\eta_{lt}$ ); and detection ( $\eta_{ld}$ ); fully secure DIQKD is possible as long as  $\eta_l = \eta_{ls}\eta_{lt}\eta_{ld} \geq 0.943$  can be attained by each user. Taking, for instance,  $\eta_l = 95\%$  (blue curves in Fig. 3), the secret key can be securely distributed over large distances while completely avoiding the transmission losses. In particular, assuming in Fig. 3 realistic<sup>34</sup>  $\eta_{lt} = e^{-L/L_{att}}$  with  $L_{att} = 22$  km, and each of the sources<sup>32</sup> to be producing photons at 100 MHz rate with  $p = 10^{-4}$ , a key rate of 1 bit/s can be attained over approximately 50 km.

### Conclusions and outlook

Two proposals for photonic implementations of DIQKD schemes have been given here. They make

use of side- or central-heralding, and utilise two or four single-photon sources, respectively. They are capable of maintaining security despite arbitrary transmission losses, and distribute keys over large distances given sufficiently high local efficiencies. While the requirements on the single-photon sources for these protocols are currently challenging, based on the rapid technological improvement and anticipated capabilities<sup>46–49</sup> of these devices we expect that the demands on fully secure DIQKD implementations presented here will soon be fulfilled.

### Methods

In standard DIQKD protocols, Alice and Bob measure their particles. A subset of these measurements is publicly announced so that the users can count how many times different outcomes ( $a, b$ ) are obtained for the different combinations of inputs ( $x, y$ ). From this information, they compute the amount of achievable secret key and, if positive, distil it by means of classical post-processing<sup>50</sup> from the remainder of data being shared, specifically, from particular pre-designed measurement settings ( $x^*, y^*$ ).<sup>2–4</sup> The attainable key rate can be then bounded by inspecting the observed single-pair behaviour  $\mathbf{p} = P(ab|xy)$  as follows:<sup>7</sup>

$$R \geq \tilde{R} = H(A|E) - H(x^*|y^*), \quad (4)$$

where  $H(x^*|y^*)$  is the classical conditional Shannon entropy between Alice and Bob outputs when choosing inputs ( $x^*, y^*$ ), while  $H(A|E)$  is the conditional von Neumann entropy between Alice’s output and the quantum state in hands of the eavesdropper, Eve.<sup>7</sup>

For a generic behaviour or a Bell inequality, the computation of  $H(A|E)$  optimised over attacks of Eve turns out to be extremely hard, and the problem has only been solved for the simplest CHSH Bell inequality.<sup>2</sup> Here, we use a lower bound on  $H(A|E)$ , which in turn provides a bound on the key rate computable for any type of correlations. It is obtained by replacing von Neumann entropy in Eq. (4) by the min-entropy.<sup>4</sup> This quantity is then directly connected to the guessing probability,  $G_{\mathbf{p}}(x^*)$ , by Eve on Alice’s outputs of measurement  $x^*$ . It can be computed for any Bell correlations exhibited by  $\mathbf{p}$  by means of semi-definite programming, as explained in App. D. The resulting bound on the key rate, which has already appeared in previous security proofs,<sup>4,5</sup> reads

$$R \geq \tilde{R} \geq R^\downarrow = -\log_2 G_{\mathbf{p}}(x^*) - H(x^*|y^*). \quad (5)$$

In an ideal scenario with two outcomes, there are no errors between Alice and Bob,  $H(x^*|y^*) = 0$ , and Eve has no information about Alice’s outputs,  $G_{\mathbf{p}}(x^*) = 1/2$ , so that  $R = R^\downarrow = 1$ . Because of its ease of computation,  $R^\downarrow$  is the quantity used here to estimate attainable key rates of the implementations proposed.

When considering protocols that incorporate a heralding stage depending on an outcome  $c$ , with

rounds occurring at a repetition rate  $\nu_{\text{rep}}$ , we quantify the effective key rate of secret bits certified per time-unit as:

$$K = \nu_{\text{rep}} p(c=\checkmark) R^\downarrow, \quad (6)$$

where  $p(c=\checkmark)$  is the probability of successful heralding in each round.

In order to obtain the key rates presented in Fig. 3, we perform an unconstrained nonlinear optimisation to maximize  $K$  over all adjustable parameters of the

schemes depicted in Fig. 2, i.e., their source parameters  $p$  and  $\bar{p}$ , transmittance values  $T$  and  $t$ , as well as polarization angles specifying the user measurements. To compute the critical values for the different noise parameters, we perform similar optimization procedures until Eq. (6) cannot be made strictly positive. Details about these optimization steps are given in Apps. D, E and F. In App. G, we also speculate about potential improvements of the attainable key rates, when Alice and Bob are further allowed to use two-way communication.

- 
- [1] D. Mayers and A. Yao, “Quantum cryptography with imperfect apparatus,” in *Proceedings of the 39th IEEE Conference on Foundations of Computer Science* (1998).
  - [2] Antonio Acín, Nicolas Brunner, Nicolas Gisin, Serge Massar, Stefano Pironio, and Valerio Scarani, “Device-Independent Security of Quantum Cryptography against Collective Attacks,” *Phys. Rev. Lett.* **98**, 230501 (2007).
  - [3] Stefano Pironio, Antonio Acín, Nicolas Brunner, Nicolas Gisin, Serge Massar, and Valerio Scarani, “Device-independent quantum key distribution secure against collective attacks,” *New J. Phys.* **11**, 045021 (2009).
  - [4] Lluís Masanes, Stefano Pironio, and Antonio Acín, “Secure device-independent quantum key distribution with causally independent measurement devices,” *Nat. Commun.* **2**, 238– (2011).
  - [5] S. Pironio, L. Masanes, A. Leverrier, and A. Acín, “Security of Device-Independent Quantum Key Distribution in the Bounded-Quantum-Storage Model,” *Phys. Rev. X* **3**, 031007 (2013).
  - [6] Umesh Vazirani and Thomas Vidick, “Fully device-independent quantum key distribution,” *Phys. Rev. Lett.* **113**, 140501 (2014).
  - [7] R. Arnon-Friedman, R. Renner, and T. Vidick, “Simple and tight device-independent security proofs,” *ArXiv e-prints* (2016), arXiv:1607.01797 [quant-ph].
  - [8] John Bell, “On the Einstein-Podolsky-Rosen Paradox,” *Physics* **1**, 195–200 (1964).
  - [9] Nicolas Brunner, Daniel Cavalcanti, Stefano Pironio, Valerio Scarani, and Stephanie Wehner, “Bell nonlocality,” *Rev. Mod. Phys.* **86**, 419–478 (2014).
  - [10] Philip M. Pearle, “Hidden-variable example based upon data rejection,” *Phys. Rev. D* **2**, 1418–1425 (1970).
  - [11] Ilja Gerhardt, Qin Liu, Antía Lamas-Linares, Johannes Skaar, Valerio Scarani, Vadim Makarov, and Christian Kurtsiefer, “Experimentally faking the violation of bell’s inequalities,” *Phys. Rev. Lett.* **107**, 170404 (2011).
  - [12] John F. Clauser, Michael A. Horne, Abner Shimony, and Richard A. Holt, “Proposed experiment to test local hidden-variable theories,” *Phys. Rev. Lett.* **23**, 880–884 (1969).
  - [13] Philippe H. Eberhard, “Background level and counter efficiencies required for a loophole-free einstein-podolsky-rosen experiment,” *Phys. Rev. A* **47**, R747–R750 (1993).
  - [14] M. A. Rowe, D. Kielpinski, V. Meyer, W. M. Itano, C. Monroe, and D. J. Wineland, “Experimental violation of a Bell’s inequality with efficient detection,” *Nature* **409** (2001).
  - [15] D. N. Matsukevich, P. Maunz, D. L. Moehring, S. Olmschenk, and C. Monroe, “Bell inequality violation with two remote atomic qubits,” *Phys. Rev. Lett.* **100**, 150404 (2008).
  - [16] Julian Hofmann, Michael Krug, Norbert Ortégel, Lea Grard, Markus Weber, Wenjamin Rosenfeld, and Harald Weinfurter, “Heralded entanglement between widely separated atoms,” *Science* **337**, 72–75 (2012).
  - [17] B. Hensen, H. Bernien, A. E. Dreau, A. Reiserer, N. Kalb, M. S. Blok, J. Ruitenbergh, R. F. L. Vermeulen, R. N. Schouten, C. Abellan, W. Amaya, V. Pruneri, M. W. Mitchell, M. Markham, D. J. Twitchen, D. Elkouss, S. Wehner, T. H. Taminiau, and R. Hanson, “Loophole-free bell inequality violation using electron spins separated by 1.3 kilometres,” *Nature* **526**, 682–686 (2015).
  - [18] Alejandro Máttar, Jonatan Bohr Brask, and Antonio Acín, “Device-independent quantum key distribution with spin-coupled cavities,” *Phys. Rev. A* **88**, 062319 (2013).
  - [19] Nicolas Brunner, Andrew B Young, Chengyong Hu, and John G Rarity, “Proposal for a loophole-free bell test based on spinphoton interactions in cavities,” *New J. Phys.* **15**, 105006 (2013).
  - [20] N. Sangouard, J.-D. Bancal, N. Gisin, W. Rosenfeld, P. Sekatski, M. Weber, and H. Weinfurter, “Loophole-free bell test with one atom and less than one photon on average,” *Phys. Rev. A* **84**, 052122 (2011).
  - [21] Marissa Giustina, Alexandra Mech, Sven Ramelow, Bernhard Wittmann, Johannes Kofler, Jorn Beyer, Adriana Lita, Brice Calkins, Thomas Gerrits, Sae Woo Nam, Rupert Ursin, and Anton Zeilinger, “Bell violation using entangled photons without the fair-sampling assumption,” *Nature* **497**, 227 – 230 (2013).
  - [22] B. G. Christensen, K. T. McCusker, J. B. Altepeter, B. Calkins, T. Gerrits, A. E. Lita, A. Miller, L. K. Shalm, Y. Zhang, S. W. Nam, N. Brunner, C. C. W. Lim, N. Gisin, and P. G. Kwiat, “Detection-loophole-free test of quantum nonlocality, and applications,”

- Phys. Rev. Lett.* **111**, 130406 (2013).
- [23] Marissa Giustina, Marijn A. M. Versteegh, Sören Wengerowsky, Johannes Handsteiner, Armin Hochrainer, Kevin Phelan, Fabian Steinlechner, Johannes Kofler, Jan-Åke Larsson, Carlos Abellán, Waldimar Amaya, Valerio Pruneri, Morgan W. Mitchell, Jörn Beyer, Thomas Gerrits, Adriana E. Lita, Lynden K. Shalm, Sae Woo Nam, Thomas Scheidl, Rupert Ursin, Bernhard Wittmann, and Anton Zeilinger, “Significant-loophole-free test of bell’s theorem with entangled photons,” *Phys. Rev. Lett.* **115**, 250401 (2015).
- [24] Lynden K. Shalm, Evan Meyer-Scott, Bradley G. Christensen, Peter Bierhorst, Michael A. Wayne, Martin J. Stevens, Thomas Gerrits, Scott Glancy, Deny R. Hamel, Michael S. Allman, Kevin J. Coakley, Shellee D. Dyer, Carson Hodge, Adriana E. Lita, Varun B. Verma, Camilla Lambrocco, Edward Tortorici, Alan L. Migdall, Yanbao Zhang, Daniel R. Kumar, William H. Farr, Francesco Marsili, Matthew D. Shaw, Jeffrey A. Stern, Carlos Abellán, Waldimar Amaya, Valerio Pruneri, Thomas Jennewein, Morgan W. Mitchell, Paul G. Kwiat, Joshua C. Bienfang, Richard P. Mirin, Emanuel Knill, and Sae Woo Nam, “Strong loophole-free test of local realism\*,” *Phys. Rev. Lett.* **115**, 250402 (2015).
- [25] Igor Aharonovich, Dirk Englund, and Milos Toth, “Solid-state single-photon emitters,” *Nat. Photonics* **10**, 631–641 (2016).
- [26] Markus Müller, Samir Bounouar, Klaus D. Jöns, M. Glässl, and P. Michler, “On-demand generation of indistinguishable polarization-entangled photon pairs,” *Nat. Photonics* **8**, 224–228 (2014).
- [27] Julien Claudon, Joel Bleuse, Nitin Singh Malik, Maela Bazin, Perine Jaffrennou, Niels Gregersen, Christophe Sauvan, Philippe Lalanne, and Jean-Michel Gerard, “A highly efficient single-photon source based on a quantum dot in a photonic nanowire,” *Nat. Photonics* **4**, 174–177 (2010).
- [28] Juan C Loredo, Nor A Zakaria, Niccolo Somaschi, Carlos Anton, Lorenzo De Santis, Valerian Giesz, Thomas Grange, Matthew A Broome, Olivier Gazzano, Guillaume Coppola, *et al.*, “Scalable performance in solid-state single-photon sources,” *Optica* **3**, 433–440 (2016).
- [29] Hui Wang, Z.-C. Duan, Y.-H. Li, Si Chen, J.-P. Li, Y.-M. He, M.-C. Chen, Yu He, X. Ding, Cheng-Zhi Peng, Christian Schneider, Martin Kamp, Sven Höfling, Chao-Yang Lu, and Jian-Wei Pan, “Near-transform-limited single photons from an efficient solid-state quantum emitter,” *Phys. Rev. Lett.* **116**, 213601 (2016).
- [30] Je-Hyung Kim, Tao Cai, Christopher J. K. Richardson, Richard P. Leavitt, and Edo Waks, “Two-photon interference from a bright single-photon source at telecom wavelengths,” *Optica* **3**, 577–584 (2016).
- [31] N. Somaschi, V. Giesz, L. De Santis, J. C. Loredo, M. P. Almeida, G. Hornecker, S. L. Portalupi, T. Grange, C. Anton, J. Demory, C. Gomez, I. Sagnes, N. D. Lanzillotti-Kimura, A. Lemaitre, A. Auffeves, A. G. White, L. Lanco, and P. Senellart, “Near-optimal single-photon sources in the solid state,” *Nat. Photonics* (2016).
- [32] Xing Ding, Yu He, Z.-C. Duan, Niels Gregersen, M.-C. Chen, S. Unsleber, S. Maier, Christian Schneider, Martin Kamp, Sven Höfling, Chao-Yang Lu, and Jian-Wei Pan, “On-demand single photons with high extraction efficiency and near-unity indistinguishability from a resonantly driven quantum dot in a micropillar,” *Phys. Rev. Lett.* **116**, 020401 (2016).
- [33] Paul G. Kwiat, Klaus Mattle, Harald Weinfurter, Anton Zeilinger, Alexander V. Sergienko, and Yanhua Shih, “New high-intensity source of polarization-entangled photon pairs,” *Phys. Rev. Lett.* **75**, 4337–4341 (1995).
- [34] Nicolas Gisin, Stefano Pironio, and Nicolas Sangouard, “Proposal for implementing device-independent quantum key distribution based on a heralded qubit amplifier,” *Phys. Rev. Lett.* **105**, 070501 (2010).
- [35] Alejandro Máttar and Antonio Acín, “Implementations for device-independent quantum key distribution,” *Phys. Scr.* **91**, 043003 (2016).
- [36] Philippe Grangier, Juan Ariel Levenson, and Jean-Philippe Poizat, “Quantum non-demolition measurements in optics,” *Nature* **396**, 537–542 (1998).
- [37] B. C. Jacobs, T. B. Pittman, and J. D. Franson, “Quantum relays and noise suppression using linear optics,” *Phys. Rev. A* **66**, 052307 (2002).
- [38] Pieter Kok, Hwang Lee, and Jonathan P. Dowling, “Single-photon quantum-nondemolition detectors constructed with linear optics and projective measurements,” *Phys. Rev. A* **66**, 063814 (2002).
- [39] Jian-Wei Pan, Dik Bouwmeester, Harald Weinfurter, and Anton Zeilinger, “Experimental entanglement swapping: Entangling photons that never interacted,” *Phys. Rev. Lett.* **80**, 3891–3894 (1998).
- [40] Marcos Curty and Tobias Moroder, “Heralded-qubit amplifiers for practical device-independent quantum key distribution,” *Phys. Rev. A* **84**, 010304 (2011).
- [41] Evan Meyer-Scott, Marek Bula, Karol Bartkiewicz, Antonín Černoch, Jan Soubusta, Thomas Jennewein, and Karel Lemr, “Entanglement-based linear-optical qubit amplifier,” *Phys. Rev. A* **88**, 012327 (2013).
- [42] Kaushik P. Seshadreesan, Masahiro Takeoka, and Masahide Sasaki, “Progress towards practical device-independent quantum key distribution with spontaneous parametric down-conversion sources, on-off photodetectors, and entanglement swapping,” *Phys. Rev. A* **93**, 042328 (2016).
- [43] David Pitkanen, Xiongfeng Ma, Ricardo Wickert, Peter van Loock, and Norbert Lütkenhaus, “Efficient heralding of photonic qubits with applications to device-independent quantum key distribution,” *Phys. Rev. A* **84**, 022325 (2011).
- [44] Mikołaj Lasota, Czesław Radzewicz, Konrad Banaszek, and Rob Thew, “Linear optics schemes for entanglement distribution with realistic single-photon sources,” *Phys. Rev. A* **90**, 033836 (2014).
- [45] Antonio Acín, Serge Massar, and Stefano Pironio, “Randomness versus nonlocality and entanglement,” *Phys. Rev. Lett.* **108**, 100402 (2012).
- [46] M. Arcari, I. Söllner, A. Javadi, S. Lindskov Hansen, S. Mahmoodian, J. Liu, H. Thyrestrup, E. H. Lee, J. D. Song, S. Stobbe, and P. Lodahl, “Near-unity coupling efficiency of a quantum emitter to a photonic

- crystal waveguide,” *Phys. Rev. Lett.* **113**, 093603 (2014).
- [47] Jake Iles-Smith, Dara P. S. McCutcheon, Ahsan Nazir, and Jesper Mrk, “Phonon limit to simultaneous near-unity efficiency and indistinguishability in semiconductor single photon sources,” *ArXiv e-prints* (2016), [arXiv:1612.04173 \[quant-ph\]](#).
  - [48] Stephen Wein, Nikolai Lauk, Roohollah Ghobadi, and Christoph Simon, “Towards room temperature indistinguishable single-photon sources using ultra-small mode volume cavities and solid-state emitters,” *ArXiv e-prints* (2017), [arXiv:1710.03742 \[quant-ph\]](#).
  - [49] Chris Gustin and Stephen Hughes, “Influence of electron-phonon scattering for an on-demand quantum dot single-photon source using cavity-assisted adiabatic passage,” *Phys. Rev. B* **96**, 085305 (2017).
  - [50] Valerio Scarani, Helle Bechmann-Pasquinucci, Nicolas J. Cerf, Miloslav Dušek, Norbert Lütkenhaus, and Momtchil Peev, “The security of practical quantum key distribution,” *Rev. Mod. Phys.* **81**, 1301–1350 (2009).
  - [51] Pieter Kok and Samuel L. Braunstein, “Postselected versus nonpostselected quantum teleportation using parametric down-conversion,” *Phys. Rev. A* **61**, 042304 (2000).
  - [52] O. Nieto-Silleras, S. Pironio, and J. Silman, “Using complete measurement statistics for optimal device-independent randomness evaluation,” *New J. Phys.* **16**, 013035 (2014).
  - [53] Miguel Navascués, Stefano Pironio, and Antonio Acín, “Bounding the set of quantum correlations,” *Phys. Rev. Lett.* **98**, 010401 (2007).
  - [54] Stephen Boyd and Lieven Vandenbergh, *Convex Optimization* (Cambridge University Press, New York, NY, USA, 2004).
  - [55] Le Phuc Thinh, Gonzalo de la Torre, Jean-Daniel Bancal, Stefano Pironio, and Valerio Scarani, “Randomness in post-selected events,” *New J. Phys.* **18**, 035007 (2016).
  - [56] Alejandro Máttar, Paul Skrzypczyk, Jonatan Bohr Brask, Daniel Cavalcanti, and Antonio Acín, “Optimal randomness generation from optical Bell experiments,” *New J. Phys.* **17**, 022003 (2015).

## Acknowledgements

We thank Rotem Arnom-Friedman, Mikołaj Lasota, Stefano Pironio and Nicolas Sangouard for helpful discussions. This work was supported by the ERC CoG QITBOX, Spanish MINECO (QIBEQI FIS2016-80773-P and Severo Ochoa SEV-2015-0522), Fundacio Cellex and Generalitat de Catalunya (SGR875 and CERCA Program), as well as by Foundation for Polish Science within the TEAM project “Quantum Optical Communication Systems” co-financed by the European Union under the European Regional Development Fund.



## Supplementary Information for

A. Máttar et al. “*Device-independent quantum key distribution with single-photon sources*”

### Appendix A: States produced by the SPDC and single-photon sources

The process of spontaneous parametric down-conversion<sup>33</sup> (SPDC) producing two-mode polarisation entangled photons is described by the Hamiltonian  $\hat{H} = i\kappa(a_H^\dagger b_V^\dagger - a_V^\dagger b_H^\dagger) + h.c.$ , where  $a_H^\dagger$ ,  $a_V^\dagger$ ,  $b_H^\dagger$  and  $b_V^\dagger$  are the bosonic creation operators of the two spatial modes  $a$  and  $b$ , with  $H$  and  $V$  denoting their orthogonal polarizations. Rewriting  $H$  with help of the  $su(1,1)$  algebra generators, i.e., ones that obey  $[L_-, L_+] = 2L_0$  and  $[L_0, L_\pm] = \pm L_\pm$ , it is straightforward to verify that the state produced via the SPDC reads:<sup>51</sup>

$$|\Psi_{\text{SPDC}}\rangle = e^{-i\hat{H}t}|0\rangle = e^{\tau(L_+ - L_-)}|0\rangle \quad (\text{A1})$$

$$= (1 - \tanh^2 \tau) e^{\tanh \tau L_+} |0\rangle, \quad (\text{A2})$$

where  $L_+ = L_-^\dagger = a_H^\dagger b_V^\dagger - a_V^\dagger b_H^\dagger$ ,  $|0\rangle$  denotes the vacuum state of all modes, while  $\tau = \kappa t > 0$  can be assumed to be real.

Moreover, as throughout this work we consider photonic schemes based on (binary, on/off) photodetection, the state  $\Psi_{\text{SPDC}}$  should be interpreted as an incoherent mixture of different photon-number states due to lack of a global phase reference. Hence, defining  $q = \tanh^2 \tau$  as the effective parameter of the SPDC process, one arrives at the expression:

$$\varrho_{\text{SPDC}} = (1 - q)^2 \sum_{n=0}^{\infty} (n+1) q^n |\Psi_n\rangle\langle\Psi_n|, \quad (\text{A3})$$

where  $|\Psi_n\rangle = \frac{1}{n!\sqrt{n+1}} L_+^n |0\rangle$  is the pure state obtained when  $n$  photon-pair excitations occur during the down-conversion.

Nonetheless, for simplicity and the purpose of our work, we redefine the state (A3) in an unnormalised,  $\text{Tr}[\sigma_{\text{SPDC}}] = 4/(2-p)^2$ , fashion as:

$$\sigma_{\text{SPDC}} = \sum_{n=0}^{\infty} \frac{n+1}{2^n} \bar{p}^n |\Psi_n\rangle\langle\Psi_n| \quad (\text{A4})$$

$$= |0\rangle\langle 0| + \bar{p} |\Psi_1\rangle\langle\Psi_1| + O(\bar{p}^2), \quad (\text{A5})$$

so that the parameter  $\bar{p} = 2q$  can now be directly associated with the contribution of the desired singlet:

$$|\Psi_1\rangle = \frac{1}{\sqrt{2}} (|1_H\rangle_a |1_V\rangle_b - |1_V\rangle_a |1_H\rangle_b) \quad (\text{A6})$$

$$= \frac{1}{\sqrt{2}} (|HV\rangle - |VH\rangle). \quad (\text{A7})$$

Experimentally, the parameter  $\bar{p}$  is kept small (below  $10^{-2}$ ) and may be adjusted with squeezing techniques.<sup>23,24</sup> Although large values of  $\bar{p}$  increase the

production rate of the target maximally entangled two-photon states,  $|\Psi_1\rangle$ , they also increase the relative contribution of spurious higher-order terms,  $|\Psi_{n>1}\rangle$ , to the SPDC process.

On the other hand, as stated in the main text, whenever the single-photon (SP) sources<sup>25</sup> are used, we represent states they produce in an analogous unnormalised,  $\text{Tr}[\sigma_{\text{SP}}] = 1/(1-p)$ , manner as:

$$\sigma_{\text{SP}} = \sum_{n=1}^{\infty} p^{n-1} |n\rangle\langle n| \quad (\text{A8})$$

$$= |1\rangle\langle 1| + p |2\rangle\langle 2| + O(p^2), \quad (\text{A9})$$

where the desired single-photon is then produced at the *zeroth* order in  $p$  – in contrast to the SPDC process (A4) in which the target photon-pair (A7) occurs at the *first* order in  $\bar{p}$  in Eq. (A5).

Finally, let us emphasise that throughout this work we perform calculations for all the schemes beyond their expected ideal working-order in  $\bar{p}$  and  $p$ , i.e., by performing truncations of (A5) and (A9) at higher orders. Still, it is crucial to mention that, when we compute the results (key rates and figures of merit presented in Table I of the main text), we nevertheless bypass such a truncation by assuming that higher-order terms (those which were dropped) are controlled by the eavesdropper to her own benefit. We give the details of this technique in App. E below.

### Appendix B: Heralded state produced by the qubit amplifier of Gisin *et al.*<sup>34</sup>

The original scheme of Ref. 34 is of the SH type (see Fig. 1(a) of the main text) and consists of an SPDC source held by Alice and two single-photon sources (emitting photons in  $H$  and  $V$  polarisation modes) held by Bob. For the sake of the argument, let us assume that all the sources do not produce multiple pairs, which is only beneficial for the scheme.

The initial composite state of Alice and Bob before communication and amplification reads:<sup>34</sup>

$$[(1 - \bar{p}) |0\rangle\langle 0| + \bar{p} |\Psi_1\rangle\langle\Psi_1|] \otimes |1_H\rangle\langle 1_H| \otimes |1_V\rangle\langle 1_V|. \quad (\text{B1})$$

Bob’s photons enter a beam-splitter of transmittance  $T$ , so that the reflected mode can then be combined with the mode received from Alice within an implementation of the Bell-state measurement (BSM). As a consequence, the final unnormalized state that is shared by Alice and Bob, conditioned on the (heralding) success of the BSM performed by Bob, reads:

$$(1 - \bar{p})(1 - T)^2 |0\rangle\langle 0| + \bar{p}\eta T(1 - T) |\Psi_1\rangle\langle\Psi_1| + \dots, \quad (\text{B2})$$

where we have already ignored all irrelevant terms that do not yield any correlations apart from the vacuum—which occurs with probability proportional to  $(1-T)^2$ , since both of Bob’s photons are reflected and detected. The second term in Eq. (B2) corresponds to the case when Alice produces the singlet (A7), which is transmitted with probability  $\eta_t$ , and only one of Bob’s photons is reflected. One can see that Eq. (B2) is of the form of Eq. (1) in the main text with the effective  $\lambda = T/(1-T)$ .

Such a feature will always emerge as long as the singlet (target) state is proportional to  $\eta_t$ , while the vacuum component remains unaffected by the finite transmission efficiency. In particular, it naturally generalises to scenarios based on entanglement-swapping<sup>40–42</sup> and hence, as explained in the main text, constitutes the main limitation of all these schemes.

### Appendix C: Heralded states produced by the SH and CH schemes

Ideally, the SH scheme depicted in Fig. 2(a) of the main text requires Alice to produce a single pair in the SPDC process and Bob to prepare two photons with independent on-demand sources. Hence, inspecting the expressions (A4) and (A8) respectively, the SH scheme ideally works at the first order in  $\bar{p}$  and the zeroth order in  $p$ . Nevertheless, we perform the analysis to the second order in both  $p$  and  $\bar{p}$ , i.e., we compute the unnormalized initial state  $\rho_{AB}^{(SH)}$  as

$$\begin{aligned} \rho_{AB}^{(SH)} = & |0, 1_H^B 1_V^B\rangle\langle\ldots| + p |0, 1_H^B 2_V^B\rangle\langle\ldots| + \\ & p |0, 2_H^B 1_V^B\rangle\langle\ldots| + p^2 |0, 2_H^B 2_V^B\rangle\langle\ldots| + \\ & p^2 |0, 1_H^B 3_V^B\rangle\langle\ldots| + p^2 |0, 3_H^B 1_V^B\rangle\langle\ldots| + \\ & \bar{p} |\Psi_1, 1_H^B 1_V^B\rangle\langle\ldots| + \\ & p\bar{p} |\Psi_1, 1_H^B 2_V^B\rangle\langle\ldots| + p\bar{p} |\Psi_1, 2_H^B 1_V^B\rangle\langle\ldots| + \\ & \frac{3}{4}\bar{p}^2 |\Psi_2, 1_H^B 1_V^B\rangle\langle\ldots| + O(p^i \bar{p}^j)_{i+j=3}. \end{aligned} \quad (C1)$$

The first six terms above are spurious, as they are related to vacuum production rounds of the SPDC source held by Alice and, in particular, the first term  $|0, 1_H^B 1_V^B\rangle$  is the dominant one in this expression. The seventh term occurs at order  $\bar{p}$  and is the desired term. The eighth and ninth terms occur at the order  $p\bar{p}$  and are related to cases in which the SPDC process succeeded but one of the single-photon sources emitted two photons. Finally the last term corresponds to a double-pair emission by the SPDC source.

The perturbative initial state (C1) undergoes the linear optics circuit of the SH scheme, illustrated in Fig. 2(a) of the main text. The evolution—which includes channel losses—is formally represented by a quantum channel  $\Lambda^{SH}$  such that  $\Lambda^{SH}(\rho_{AB}^{(SH)})$  is the

quantum state right before photodetection. If  $\Pi_{\checkmark}^C$  denotes the measurement element corresponding to the detection of two orthogonal polarizations within the BSM, then the heralded state shared by Alice and Bob reads:

$$\rho_{AB|\checkmark}^{(SH)} = \text{Tr}_C \left[ \Lambda^{SH} \left( \rho_{AB}^{(SH)} \right) \mathbb{1}^A \otimes \mathbb{1}^B \otimes \Pi_{\checkmark}^C \right]. \quad (C2)$$

Although we omit here the explicit expression for the above state when substituting for  $\rho_{AB}^{(SH)}$  according to Eq. (C1), its form simplifies to Eq. (2) stated in the main text after truncating  $\rho_{AB|\checkmark}^{(SH)}$  to the first order.

As far as the CH scheme is concerned, the ideal state distribution occurs at the zeroth order in  $p$ , that is, when each of the four photon sources produces a single photon. Still, when working to the first order, the initial state reads:

$$\begin{aligned} \rho_{AB}^{(CH)} = & |1_H^A 1_V^A, 1_H^B 1_V^B\rangle\langle\ldots| + p |1_H^A 1_V^A, 1_H^B 2_V^B\rangle\langle\ldots| + \\ & p |1_H^A 1_V^A, 2_H^B 1_V^B\rangle\langle\ldots| + p |1_H^A 2_V^A, 1_H^B 1_V^B\rangle\langle\ldots| + \\ & p |2_H^A 1_V^A, 1_H^B 1_V^B\rangle\langle\ldots| + O(p^2). \end{aligned} \quad (C3)$$

In a similar manner to the SH scheme, the state (C3) undergoes the evolution illustrated in Fig. 2(b) of the main text, which is represented by the channel  $\Lambda^{CH}$  yielding  $\Lambda^{CH}(\rho_{AB}^{(CH)})$  as the quantum state right before photodetection. The heralded state is then described by an equation analogous to Eq. (C2), yet, as before, we omit here its explicit form. However, the full expression for  $\rho_{AB|\checkmark}^{(CH)}$  simplifies to Eq. (3) of the main text, when computed to the zeroth order.

### Appendix D: Guessing probability

The min-entropy term  $-\log_2 G_{\mathbf{p}}(x^*)$  in Eq. (5) of the main text is expressed with help of the *device-independent guessing probability*, i.e., the average probability that the eavesdropper Eve correctly guesses the output of Alice using an optimal strategy:<sup>52</sup>

$$\begin{aligned} G_{\mathbf{p}}(x^*) := & \max_{\{\mathbf{p}^e\}} \sum_e P(e) P(a = e|x^*, e) \quad (D1) \\ \text{s.t.} \quad & \sum_e \mathbf{p}^e = \mathbf{p} \text{ and } \forall e: \mathbf{p}^e \in \tilde{Q}. \end{aligned}$$

Here,  $P(e)$  denotes the probability that Eve observes the outcome  $e$ , while  $P(a = e|x^*, e)$  effectively represents the probability that Alice obtains an outcome  $a$  coinciding with  $e$ , given to be the one observed by Eve.

Any strategy of Eve in Eq. (D1) can be seen as a measurement that she performs on her system, which

then produces a decomposition (a collection) of unnormalized behaviours  $\{\mathbf{p}^e\}$  distributed between Alice and Bob. Guessing probability (D1) is then obtained by maximising the success of Eve's strategy over all such possible decompositions that, however, must reproduce on average the behaviour  $\mathbf{p}$  observed by Alice and Bob and be compatible with quantum mechanics (see the second line of Eq. (D1)). Formally, each of them must belong to the set of unnormalised behaviours  $\tilde{Q}$  which stem from the Born's rule when valid quantum measurements act on an unnormalized, yet unspecified, quantum state. Thus, to enforce the *quantumness* of Eve's strategy, the second constraint in Eq. (D1) demands that all  $\mathbf{p}^e$  belong to  $\tilde{Q}$ .

Imposing membership in  $\tilde{Q}$  is difficult since a precise characterization of  $\tilde{Q}$  is unknown. However, semi-definite programming (SDP) relaxations similar to the ones presented by Navascués *et al.*<sup>53</sup> can be introduced to bound  $G_{\mathbf{p}}(x^*)$  from above.<sup>52</sup> One defines a convergent hierarchy of convex sets that have a precise characterization and obey  $\tilde{Q}_1 \supseteq \tilde{Q}_2 \supseteq \dots \supseteq \tilde{Q}$ . This hierarchy approximates the quantum set  $\tilde{Q}$  from outside, so that any optimisation over the quantum set can be relaxed (to some order  $k$ ) by replacing  $\tilde{Q}$  in Eq. (D1) with  $\tilde{Q}_k$ . Hence, the program presented in Eq. (D1) becomes an SDP when relaxations of the set  $\tilde{Q}$  are employed—in our work we mostly consider relaxations to the order  $1 + AB$ , i.e., an intermediary order between first and second orders.

Finally, let us note that from the dual formulation<sup>54</sup> of the SDP program employed, we are also always able to retrieve the Bell inequality that is optimal for bounding the degree of predictability that a quantum eavesdropper may have about the string of Alice's outcomes.<sup>52</sup>

### Appendix E: Dealing with higher-order multi-photon contributions

In order to deal with quantum states produced by SPDC and single-photon sources (presented in App. C), one typically truncates the global state produced by all sources in the setup up to a certain order  $n$ .<sup>34,40,41</sup> Since any setup we consider is powered by SPDC sources parameterized by  $\bar{p}$  and single-photon sources parametrized by  $p$ , a truncation to the order, e.g.,  $n = 2$  of the global state—which is the tensor product of the states of each source—would keep all terms up to order  $O(p^2)$ ,  $O(p\bar{p})$  and  $O(\bar{p}^2)$ .

Nevertheless, this perturbative approximation may yield misleading conclusions about the nonlocal character of the observed correlations and compromise DIQKD security for a given setup. In fact, one has to guarantee that contributions not considered in the truncation will not contradict the conclusions about the nonlocal character of the behaviour in question.

To avoid this problem, we develop here a method based on SDP techniques where all high-order contributions ( $> n$ ) that are not taken into account are fully controlled by Eve, to her benefit. This may seem too conservative, but the method turns out to be efficient and not overly pessimistic, since the contribution of high-order terms becomes irrelevant for sufficiently low values of  $p$  and  $\bar{p}$ .

The key idea is to conceive higher-order contributions as producing an unknown and uncharacterized quantum behaviour  $\mathbf{p}_Q$  prepared by Eve for Alice and Bob. If  $\mathbf{p}_n^{\text{est}}$  denotes the estimation of the behaviour of Alice and Bob constructed to the order  $n$  (e.g., one derived basing on states (C1) or (C3) for SH and CH-schemes, respectively), then the first step of the method is to write the observed behaviour  $\mathbf{p}$  as a convex decomposition:  $\mathbf{p} = (1 - \epsilon_n)\mathbf{p}_n^{\text{est}} + \epsilon_n\mathbf{p}_Q$ .

At the quantum level, the total state being shared, given a collection of sources producing a perturbative state such as (A4), may be written as a convex mixture  $p(n)\rho_n + p(\bar{n})\rho_{\bar{n}}$ , where  $\rho_n$  is the truncated state according to the estimation made at some order  $n$ .  $\rho_{\bar{n}}$  is thus the remaining “tail” of high-order contributions, and  $p(\bar{n}) = 1 - p(n)$ . Moving to the level of probability distributions, linearity of Born's rule with respect to  $\rho$  implies that the elements of the observed behaviour  $\mathbf{p}$  conditioned on the outcome  $c$  employed in the heralding stage (see App. C) may be decomposed in a similar fashion, i.e.:

$$P(a, b|c) = p(n|c) P(a, b|c, n) + p(\bar{n}|c) P(a, b|c, \bar{n}). \quad (\text{E1})$$

The probabilities  $P(a, b|c, n)$  above are then nothing but the elements of the estimated behaviour  $\mathbf{p}_n^{\text{est}}$  computed up to the  $n$ th order.

We rewrite  $p(n|c)$  employing the Bayes rule:

$$p(n|c) = \frac{p(c|n)p(n)}{p(c)}. \quad (\text{E2})$$

The numerator in Eq. (E2) is known, as  $p(c|n)$  is merely the probability of observing the heralding outcome  $c$  while assuming the  $n$ th order truncation at the level of the sources. The denominator, however, is unknown and corresponds to the probability of observing the outcome  $c$ , without assuming any truncation.

Still, it is possible to set an upper bound on  $p(c)$ :

$$\begin{aligned} p(c) &= \sum_{\vec{k}=\vec{0}}^{\infty} p(\vec{k})p(c|\vec{k}) \\ &\leq p_{\vec{K}_n}(c) := \sum_{\vec{k}=\vec{0}}^{\vec{K}_n} p(\vec{k})p(c|\vec{k}) + \sum_{\vec{k} > \vec{K}_n}^{\infty} p(\vec{k}), \end{aligned} \quad (\text{E3})$$

where the vector of variables  $\vec{k} = (k_1, k_2, \dots, k_s)$  describes the possible number of photons produced by each of the  $s$  sources. In particular,  $p(\vec{k})$  gives the distribution for each of the possible combinations of photons (or photon pairs) occurring, when produced by

the sources. Vector  $\vec{K}_n$  contains the numbers of photons that each source can maximally produce, given a particular order  $n$  of the truncation.

Bounding Eq. (E2) with help of Eq. (E3), one gets the desired upper bound on  $\epsilon_n = 1 - p(n|c)$ , i.e.,

$$\epsilon_n \leq \epsilon_n^\uparrow := 1 - \frac{p(c|n)p(n)}{p_{\vec{K}_n}(c)}, \quad (\text{E4})$$

which can be importantly computed for a given optical scheme and the order  $n$  assumed. Consistently,  $\epsilon_n^\uparrow$  (and, hence,  $\epsilon_n$ ) goes to zero as the order  $n$  increases, so that  $\mathbf{p}_n^{\text{est}}$  converges to  $\mathbf{p}$  in the limit  $n \rightarrow \infty$ .

In an analogous way to Eq. (D1), we define the *device-independent guessing probability to the order  $n$  as*:

$$\begin{aligned} G_{\mathbf{p}_n^{\text{est}}}(x^*, \epsilon) &:= \max_{\{\mathbf{p}^e\}} \sum_e P(e, a = e|x^*) \\ \text{s.t. } \sum_e \mathbf{p}^e &= (1 - \epsilon)\mathbf{p}_n^{\text{est}} + \epsilon\mathbf{p}_Q, \\ \mathbf{p}_Q &\in Q \text{ and } \forall e : \mathbf{p}^e \in \tilde{Q}, \end{aligned} \quad (\text{E5})$$

where  $(\tilde{Q})Q$  denotes the set of (un)normalized quantum behaviours. The crucial difference between Eqs. (D1) and (E5) is that Eve is now *not* obliged to reproduce exactly the behaviour  $\mathbf{p}$  with her collection of unnormalised behaviours  $\{\mathbf{p}^e\}$ . Instead, she possesses a supplementary quantum behaviour  $\mathbf{p}_Q$  that she can tailor, so that it is easier for her to reproduce the behaviour  $\mathbf{p}_n^{\text{est}}$  for a given *fixed* value of  $\epsilon$  and, hence, better guess the outcome of Alice's box.

Now, the following inequalities must hold:

$$G_{\mathbf{p}_n^{\text{est}}}(x^*) \leq G_{\mathbf{p}_n^{\text{est}}}(x^*, \epsilon_n) \leq G_{\mathbf{p}_n^{\text{est}}}(x^*, \epsilon_n^\uparrow), \quad (\text{E6})$$

where the first one is guaranteed to be saturated whenever it is optimal to set  $\mathbf{p}_Q = \mathbf{p}_n^{\text{est}}$  in Eq. (E5) (i.e., the truncation plays no role), while the second one whenever the bound (E4) is tight. As a result, we may always upper-bound Eve's optimal guessing probability by  $G_{\mathbf{p}_n^{\text{est}}}(x^*, \epsilon_n^\uparrow)$ , and by doing so we can only underestimate the attainable key rate of the DIQKD protocol—see Eq. (5) of the main text.

Let us stress that the method presented above is quite general, as it can be applied to any other uncharacterised imperfection parametrised by  $\epsilon$ , such that its action arises as convex decomposition of the form  $\mathbf{p} = (1 - \epsilon)\mathbf{p}^{\text{est}} + \epsilon\mathbf{p}_Q$ . In particular, it allows to upper-bound the guessing probability for any type of noise that may be represented as a convex mixture at the level of a quantum state, given that the corresponding mixing probability can also be bound from above by a known  $\epsilon^\uparrow < 1$ .

#### Appendix F: Noise robustness for nonlocality

We analyze the robustness to white noise of the estimated behaviours  $\mathbf{p}^{\text{est}}$  that our two schemes pro-

duce. We determine the maximal value  $w^*$  of white noise  $\mathbf{1}_\mathbf{p}$ —a distribution in which all the outcomes are equally likely, independently of the measurement choices—which can be convexly added such that the behaviour  $(1 - w)\mathbf{p}^{\text{est}} + w\mathbf{1}_\mathbf{p}$  remains nonlocal.

Membership of a probability distribution to the set of local behaviours<sup>9</sup> is an instance of a linear program.<sup>54</sup> Geometrically speaking, the set of local behaviours is a polytope in the space of probability distributions, whose extremal points correspond to particular deterministic strategies  $\{\mathbf{D}_\mu\}_\mu$  that are sufficient to decompose any local behaviour. In fact, there is a finite number of such deterministic strategies, and the white noise tolerance of  $\mathbf{p}^{\text{est}}$  is given by the solution of the following linear program:

$$\begin{aligned} w^* &= \min_{\{q_\mu\}} w \\ \text{s.t. } (1 - w)\mathbf{p}^{\text{est}} + w\mathbf{1}_\mathbf{p} &= \sum_\mu q_\mu \mathbf{D}_\mu, \\ \sum_\mu q_\mu &= 1 \text{ and } \forall \mu : q_\mu \geq 0. \end{aligned} \quad (\text{F1})$$

The white-noise tolerance threshold,  $w^*$ , should be interpreted as deviations from the desired correlations at the level of probability distributions. This is the worst-case approach in which the experimental imperfections not accounted for in  $\mathbf{p}^{\text{est}}$  provide Alice and Bob with completely uncorrelated results. The fact that our schemes tolerate high amounts of white noise (see Table I of the main text) ensures that our results will not be strongly affected when introducing other sources of noise, not accounted for in the analysis.

#### Appendix G: Potential improvements by post-processing

In this last section, we would like to explore potential improvements on DIQKD implementations using post-processing techniques based on two-way communication. We don't provide any security proof, but speculate about how one could hope to relax the strong experimental requirements needed for DIQKD. Clearly, the most demanding factor in our setup is the high local efficiency  $\eta_l$  required for security, of the order of 95%. As explained in the main text, this is much higher than the local efficiency required to observe a Bell violation, which is of the order of 66%. This is because losses not only affect the observed Bell violation, and therefore Eve's predictability in Eq. (5) of the main text, but also the errors between the honest users increase, quantified by the  $H(A|B)$  term in Eq. (5). We discuss here how this effect could possibly be mitigated.

For simplicity, consider an idealised situation in which losses are the only source of errors. Then, if Alice and Bob announce and keep only the outcomes when they both detected a photon, the correlations



between them in the resulting lists are perfect, that is,  $H(A|B) = 0$ . If now one was able to establish a non-trivial bound on Eve's predictability of Alice's symbols after discarding the no-detection events as a function of initial correlations, one could hope to distill a secret key for smaller values of local efficiency,  $\eta$ , as this parameter would not have an effect on the correlations between Alice and Bob. In what follows, we adapt the techniques of Thinh *et al.*<sup>55</sup> to provide a quantification of how much randomness could be left on Alice's outputs after the honest users discard the no-detection events.

However, it is important to stress that, although such a procedure does *not* correspond to *naïve post-selection* opening the detection loophole<sup>10</sup> as the control of Eve over the *full* behaviour is, in principle, accounted for, at no point a valid security proof is provided. In fact, the authors of Ref. 55 have shown that while their techniques allow to establish a bound on the predictability of outputs after discarding the no-detection events, that is, valid in an independent and identically distributed (i.i.d.) realisation, the bound is generally not valid in non-i.i.d. scenarios. We expect the same considerations apply to our derivation below. Still, even if not general, the obtained lower bounds on key rates remain positive for smaller values of local efficiencies, suggesting that this could be a promising way of relaxing the experimental requirements for DIQKD implementations.

#### a. Conditional entropy in the presence of losses

We start by analysing the impact of the post-processing technique<sup>55</sup> on the correlations observed by Alice and Bob. We assume that the heralding measurement has succeeded and, hence, Alice and Bob have successfully received their share of the state. Thus, only local losses have to be considered, parametrised by the local efficiency  $\eta$ .

Suppose that Alice and Bob retrieve two conclusive outcomes 0, 1 and one inconclusive (lossy) outcome  $\phi$ . In the case of finite  $\eta < 1$ , the joint probability distribution of outcomes  $a$  and  $b$  conditioned on the choice of measurements  $x^*$  and  $y^*$  is given by:

$$P(ab|x^*y^*) = \begin{array}{c|ccc} & b=0 & b=1 & b=\phi \\ \hline a=0 & \eta_l^2 P(00) & \eta_l^2 P(01) & \frac{\eta_l(1-\eta_l)}{2} \\ a=1 & \eta_l^2 P(10) & \eta_l^2 P(11) & \frac{\eta_l(1-\eta_l)}{2} \\ a=\phi & \frac{\eta_l(1-\eta_l)}{2} & \frac{\eta_l(1-\eta_l)}{2} & (1-\eta_l)^2 \end{array}, \quad (\text{G1})$$

where we have dropped conditioning on  $x^*$  and  $y^*$  of terms  $P(00)$ ,  $P(01)$ ,  $P(10)$  and  $P(11)$  in the table.

Considering the full distribution (G1), the condi-

tional entropy (Eq. (5) of the main text) is given by:

$$H(x^*|y^*) = - \sum_{ab} P(ab|x^*y^*) \log_2 \frac{P(ab|x^*y^*)}{P(b|y^*)}, \quad (\text{G2})$$

so that substituting for all the entries and assuming that the outcomes 0 and 1 locally occur with equal probability, one arrives at:

$$H(x^*|y^*) = \eta_l^2 H_K(x^*|y^*) + \eta_l(1-\eta_l) + h(\eta_l), \quad (\text{G3})$$

where  $h(x) = -x \log_2(x) - (1-x) \log_2(1-x)$  is the binary entropy function, while  $H_K(x^*|y^*)$  is the conditional entropy computed only from the probability distribution of conclusive events, i.e., from outcomes within the set  $\mathcal{K} = \{(a,b)|a \neq \phi \text{ \& } b \neq \phi\}$ .

Since  $H_K(x^*|y^*) \geq 0$ , one may construct a lower-bound on  $H(x^*|y^*)$  that reads

$$H(x^*|y^*) \geq \eta_l(1-\eta_l) + h(\eta_l) \quad (\text{G4})$$

and, despite being behaviour-independent, is strictly positive for any  $\eta_l < 1$ . This shows the detrimental effects of losses on the correlations between Alice and Bob. Moreover, the bound (G4) is tight when  $H_K(x^*|y^*) = 0$ , i.e., when Alice and Bob observe perfect correlations within the subset of conclusive outcomes.

On the other hand, when Alice and Bob simply discard the no-detection events, their *post-selected* correlations are just given by  $H_K(x^*|y^*)$ . In the ideal case of a maximally entangled state affected only by losses, this term is equal to zero, as the lists of conclusive outcomes 0 and 1 are perfectly correlated.

#### b. Guessing probability with data post-processing

In order to obtain an intuition about how the post-processing method of Thinh *et al.*<sup>55</sup> could help, we will take for granted that the bound on key rate stated in Eq. (5) of the main text also holds for the list of outputs after Alice and Bob discard their no-detection events. Again, we don't expect this to be true in general, but we believe the resulting calculation has some value and suggests future research directions to strengthen DIQKD implementations.

In what follows, similarly to the scenario in which one aims to certify randomness from the post-processed data,<sup>55</sup> we provide a method to quantify Eve's predictability on Alice's symbols—her guessing probability discussed in App. D—when restricting to a particular subset of outcomes. After plugging the so-obtained guessing probability into Eq. (5), we see how, in some situations, this method allows to maintain a strictly positive secret key rate for lower values of local efficiency,  $\eta$ , which cannot be reached when utilising initial correlations exhibited by the full behaviour.

Intuitively, the price one has to pay when discarding data is a cutback in the total key rate, since more rounds must be rejected as  $\eta$  is diminished. Surprisingly, we show that this intuition is incorrect and observe cases in which the post-processing method leads to an increase in the secret key rate.

Let  $\mathcal{K} = \mathcal{K}_A \times \mathcal{K}_B$  be some product subset of  $\mathcal{O}_A \times \mathcal{O}_B$ , the set of outcomes  $(a, b)$ . We are interested in keeping only those rounds for which the outcomes  $(a, b)$  belong to  $\mathcal{K}$ . In particular,  $\mathcal{K}$  may represent the subset of conclusive outcomes, but let us emphasise that the reasoning we present is general, and works for any choice of subsets  $\mathcal{K}_A$  and  $\mathcal{K}_B$ .

Here, we consider that, once the measurement outcomes are registered, the classical information about whether  $(a, b) \in \mathcal{K}$  is publicly announced. From a practical point of view, such information can be made public at the end of the protocol, with Alice and Bob announcing whether or not  $(a, b) \in \mathcal{K}$  for each round, but without revealing the actual values of  $a$  and  $b$ . In this way, if  $(a, b) \in \mathcal{K}$ , Alice and Bob keep the round in question, while otherwise they discard it. From the security point of view, the information about whether or not  $(a, b) \in \mathcal{K}$  could have been pre-set by Eve.

We define the probability for Alice and Bob to observe an outcome belonging to the set  $\mathcal{K}$  as

$$P(\mathcal{K}) = \sum_{(a,b) \in \mathcal{K}} P(a, b | x^*, y^*) \quad (\text{G5})$$

and, for simplicity, drop its dependence on  $x^*$  and  $y^*$  that are fixed. After Alice and Bob's measurements  $x^*$  and  $y^*$  are applied on  $\text{Tr}_E \rho_{ABE}$ , the ‘‘classical-classical-quantum’’ state is given by:

$$\rho_{ABE}^{x^* y^* \mathcal{K}} = \sum_{a,b} P(a, b | x^*, y^*, \mathcal{K}) |a, b\rangle \langle a, b| \otimes \rho_E^{abx^* y^* \mathcal{K}} \quad (\text{G6})$$

where  $\rho_E^{abx^* y^* \mathcal{K}}$  denotes the quantum state of Eve that is conditioned both on the observed outcomes  $(a, b)$  belonging to  $\mathcal{K}$  and on the settings  $(x^*, y^*)$ .

Let  $\{M_{e|z}\}$  be the positive operator-valued measure representing the measurement with setting  $z$  that Eve performs on  $\rho_E^{abx^* y^* \mathcal{K}}$ . Then, according to Born's rule, it follows that  $P(e | a, b, x^*, y^*, \mathcal{K}, z) = \text{Tr}[\rho_E^{abx^* y^* \mathcal{K}} M_{e|z}]$ . The device-independent guessing probability is then defined analogously to Eq. (D1), as the probability for Eve to correctly guess the outcome  $a$  maximized over: all her measurement settings  $z$ , and over all possible quantum realizations of the distribution shared with Alice and Bob, so that its marginal correctly reproduces  $\mathbf{p} = P(a, b | x, y)$ :

$$G_{\mathbf{p}}(x^*, y^* | \mathcal{K}) = \max_{a,b} \sum_{a,b} P(a, b | \mathcal{K}) P(e = a | a, b, \mathcal{K}), \quad (\text{G7})$$

where we dropped the dependence on settings  $x^*, y^*$  and optimal  $z^*$  that are fixed within the discussion.

By applying the Bayes rule,

$$P(e | a, b, \mathcal{K}) = \frac{P(e | \mathcal{K}) P(a, b | \mathcal{K}, e)}{P(a, b | \mathcal{K})}, \quad (\text{G8})$$

we rewrite Eq. (G7) as:

$$G_{\mathbf{p}}(x^*, y^* | \mathcal{K}) = \max_{e,b} \sum_{e,b} P(e | \mathcal{K}) P(a = e, b | \mathcal{K}, e), \quad (\text{G9})$$

and, similarly, after further acknowledging that

$$P(e | \mathcal{K}) = \frac{P(e) P(\mathcal{K} | e)}{P(\mathcal{K})}, \quad (\text{G10})$$

$$P(a = e, b | \mathcal{K}, e) = \frac{P(a = e, b, \mathcal{K} | e)}{P(\mathcal{K} | e)}, \quad (\text{G11})$$

we further rewrite Eq. (G9) as:

$$\begin{aligned} G_{\mathbf{p}}(x^*, y^* | \mathcal{K}) &= \\ &= \max \frac{1}{P(\mathcal{K})} \sum_{e,b} P(e) P(a = e, b, \mathcal{K} | e) \\ &= \max \frac{1}{P(\mathcal{K})} \sum_{(e,b) \in \mathcal{K}} P(e) P(a = e, b | e). \end{aligned} \quad (\text{G12})$$

Finally, assuming the i.i.d. scenario to apply,<sup>55</sup> we obtain the local<sup>56</sup> probability of Eve correctly guessing the outcome of Alice, given that Alice and Bob select outcomes from the predefined set  $\mathcal{K}$  with *all* their outcomes being distributed according to the behaviour  $\mathbf{p}$  as:

$$\begin{aligned} G_{\mathbf{p}}(x^*, y^* | \mathcal{K}) &= \max_{\{\mathbf{p}^e\}} \frac{1}{P(\mathcal{K})} \sum_{(e,b) \in \mathcal{K}} p(e, a = e, b) \\ &\text{s.t. } \sum_e \mathbf{p}^e = \mathbf{p} \text{ and } \forall_{e \in \mathcal{K}_A} : \mathbf{p}^e \in \tilde{\mathcal{Q}}, \end{aligned} \quad (\text{G13})$$

which can be further recast into an SDP by performing relaxations, as in App. D.

### c. DIQKD with data post-processing

We substitute both the conditional entropy  $H_{\mathcal{K}}(x^* | y^*)$  and guessing probability (G13) established above into the bound (5) of the main text that we assume to hold despite the post-processing step (yet, not for non-i.i.d. attacks<sup>55</sup>) and read

$$R_{\text{pp}}^{\downarrow} = -\log_2 G_{\mathbf{p}}(x^*, y^* | \mathcal{K}) - H_{\mathcal{K}}(x^* | y^*), \quad (\text{G14})$$

where the subscript ‘‘pp’’ indicates that post-processing took place. Critically, and in sound contrast with the standard secret key bound,  $R^{\downarrow}$  in Eq. (5), one may, in principle, choose  $\mathcal{K}$  to contain

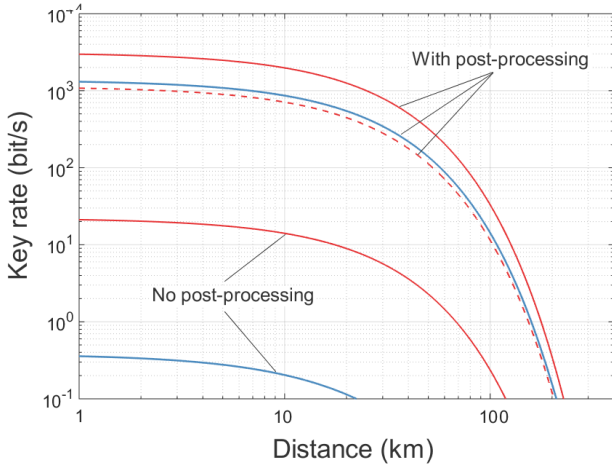


FIG. 4. **DIQKD key rates attained with 95% local efficiencies and post-processing.** The curves in red (blue) show the key rates (in bits per second) attained by the CH (SH) scheme. For the bottom curves the secret key is extracted optimising the protocol within the standard DIQKD setting, while the upper curves also include the post-processing technique that then yields a considerable increase of the corresponding key rates. Each key rate is adequately optimised over all adjustable physical parameters, yet in the case of the single-photon sources impurity parameter the lowest possible value is always favoured. Hence, we set  $p = 10^{-4}$  while computing all the solid curves while we choose  $p = 10^{-2}$  in case of the dashed curve to more adequately refer to current experimental implementations. In the latter case, only the CH scheme with post-processing employed provides a positive and a high key rate. In all cases we consider the repetition rate of photon extraction to be 100 MHz.<sup>31</sup>

perfectly correlated outcomes, so that the conditional entropy  $H_K(x^*|y^*)$  now vanishes for any value of  $\eta_l$ .

When computing  $R_{pp}^\downarrow$  for the proposed CH scheme, the post-processing method allows for the critical local efficiency,  $\eta_l^*$ , to be lowered from 94.3% (presented in Table I of main text) to 90.3%. A similar decrease is observed for the SH scheme, from 94.9% to 91.1%. The intuition behind such a drop in case of the CH scheme is that, since almost no vacuum pro-

ductions occur at the level of the sources, the inconclusive events arise primarily due to presence of local losses. As a result, hardly any information is lost when the inconclusive outcomes are discarded, which constitutes the main ingredient of the post-processing technique.

In Fig. 4, we present the attainable key rates when assuming local efficiencies of 95% in both Alice and Bob labs. As in the main text, we take the channel attenuation length of  $L_{att} = 22 \text{ km}^{-1}$ , and an efficiency for the detectors used for heralding (including both coupling and detection efficiency) of 85%. Upon optimization, we find that the parameters  $T = 0.004$  and  $t = 0.698$  yield the highest DIQKD rates for the CH scheme, and  $T = 0.025$  and  $t = 0.708$  respectively when allowing for post-processing. Interestingly, the post-processing method outperforms the standard DIQKD approach also in terms of the rates attainable. In particular, for a distance  $L = 50 \text{ km}$ , with  $p = 10^{-4}$  we certify 320.8 secret bits per second with post-processing and only 2.3 secret bits per second without it.

Our analysis also allows us to study the effect of imperfections in the single-photon sources. In contrary to the SPDC sources that always yield a zero rate for small values of the parameter  $\bar{p}$ , when optimizing the value of parameter  $p$  (describing single-photon source imperfections) its lowest possible value is always favoured. When fixing  $p$  to be small, e.g.,  $p = 10^{-4}$  (solid curves in Fig. 4), the CH scheme outperforms the SH scheme, but the improvement is not substantial. However, for more realistic values reachable in current experiments<sup>31,32</sup> higher-order photon terms start to contribute and the CH scheme becomes the *only* one to yield positive key rates, e.g., at  $p = 10^{-2}$  (dashed curve in Fig. 4) for which the CH scheme produces 112.4 secret bits per second over  $L = 50 \text{ km}$ .

Despite the caveats in the security proofs,<sup>55</sup> we expect that the promising results of this qualitative analysis could boost research in the direction of understanding how to deal with losses in realistic DIQKD implementations.